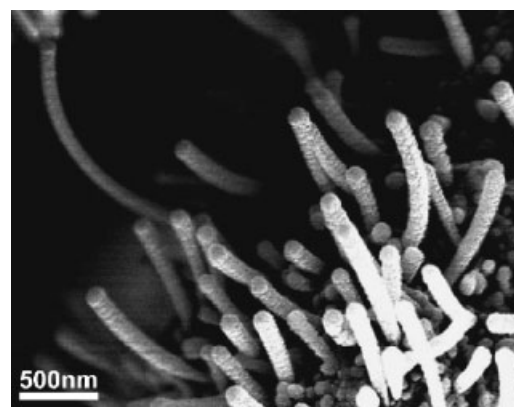


# Factors that Contribute to the Growth of Ag@TiO<sub>2</sub> Nanofibers by Plasma Deposition

Ana Borrás, Ángel Barranco, Juan P. Espinós, José Cotrino,  
Juan P. Holgado, Agustín R. González-Elipe\*

A model experiment on the plasma deposition of TiO<sub>2</sub> on silver is described which can help to identify the factors that control the formation of supported Ag@TiO<sub>2</sub> nanofibers during plasma deposition of TiO<sub>2</sub> at  $T > 130$  °C. The plasma oxidation of silver and the plasma deposition of TiO<sub>2</sub> on dispersed metal particles have also been studied and correlated with film topography. The species in the plasma have been analysed and fiber growth has been followed as a function of deposition time. The experimental evidence indicates that factors controlling fiber formation include silver mobility, stress relaxation of oxidized silver surfaces, chemical reduction of silver oxide, and inhomogeneities of the plasma sheath.



## Introduction

Nanometer-scale rods, fibers, or similar nanostructures of oxide materials, in particular TiO<sub>2</sub>, are usually prepared by means of chemical or electrochemical routes.<sup>[1–7]</sup> Methods that use liquid solutions have also been used for the synthesis of Ag core-shell TiO<sub>2</sub> composite nanofibers.<sup>[8]</sup> Heating metallic Ti and other high temperature related procedures have also been utilized for the preparation of

this type of nano-structure.<sup>[9]</sup> All these methods follow successive steps that involve drying, heating, or annealing at high temperature. The need of such types of treatments may hamper the use of these methods when mild conditions are a requisite or when the synthesis has to be carried out in a single experimental set-up. These shortcomings can be circumvented by plasma-enhanced chemical vapour deposition (PECVD). This method works at virtually any temperature and permits the synthesis of complex nanostructures without any thermal post-treatment. Carbon nanotubes (CNTs) constitute a clear example of the use of electrical discharges or plasmas for the synthesis of nanostructures at relatively low temperatures as compared with ceramic or hydrothermal processes.<sup>[10–12]</sup> Some works in the literature also account for the preparation of fibers or rods of other materials by using plasmas as the main experimental tool. For example, ZnO has been prepared in the form of aligned nanorods by combining plasmas with the heating of the substrate at temperatures of the order of 700 °C.<sup>[13]</sup> Nb<sub>2</sub>O<sub>5</sub> nanowires have been prepared by interaction of a Nb surface with a

A. Borrás, Á. Barranco, J. P. Espinós, J. Cotrino, J. P. Holgado,  
A. R. González-Elipe

Instituto de Ciencia de Materiales de Sevilla, Avda. Américo  
Vespucio 49, 41092 Sevilla, Spain

E-mail: arge@icmse.csic.es

J. P. Espinós

Departamento de Química Inorgánica, Universidad de Sevilla,  
Avda. Reina Mercedes s/n, Sevilla, Spain

J. Cotrino

Departamento de Física Atómica Molecular y Nuclear, Universi-  
dad de Sevilla, Avda. Reina Mercedes s/n, Sevilla, Spain

plasma of oxygen.<sup>[14]</sup> A He/O plasma and a complex methodology has also been used for the preparation of titanium fullerene oxides on surfaces of TiO<sub>x</sub> materials.<sup>[15]</sup> Another plasma-related approach is the synthesis of silica fibers with embedded gold particles prepared by combining plasma and heating treatments.<sup>[16]</sup>

Recently, we have reported on the preparation of a large concentration of supported Ag@TiO<sub>2</sub> core-shell nanofibers by a method based on the plasma deposition (i.e., PECVD) of titanium oxide on a complex-shaped silver substrate at  $T > 130$  °C.<sup>[17]</sup> In this previous publication we reported the phenomenology of the procedure and a first characterization of the nanofibers formed at different temperatures of the substrate. Fibres of several micrometers length and a thickness that varied between 30 and 400 nm were produced by this method. In all cases a monocrystalline silver thread  $\approx 20$  nm thick was formed in the centre of the Ag@TiO<sub>2</sub> core-shell nanofibers. In addition, based on the morphology and other characteristics of these nano-fibers, it was proposed that they form according to a new 'volcano'-type mechanism.

To explain this mechanism, in the present work we have tried to gain a deeper insight into the physical phenomena that may control the formation of the supported nanofibers. With this aim, we have performed a series of experiments by X-ray photoemission spectroscopy (XPS), optical emission spectroscopy (OES), and scanning electron microscopy (SEM). The studied systems have been specifically prepared to address and demonstrate specific issues of this 'volcano'-type mechanism. Thus, SEM analysis has been used to characterize the final morphologies of three different systems, namely: i) TiO<sub>2</sub> layers plasma deposited on complex substrates formed by a silicon wafer with small Ag or Pt particles on its surface, ii) a flat silver foil subjected to plasma oxidation for increasing periods of time, and iii) Ag@TiO<sub>2</sub> nanofibers formed on the complex-shaped silver substrate as a function of deposition time. 'In situ' XPS has been used to carry out a model experiment consisting of the plasma growth of TiO<sub>2</sub> on an oxidized silver foil. Meanwhile, OES has provided information about the type of titanium species formed in the plasma during deposition. From the experimental evidence obtained some clues are deduced that have served to understand some of the factors that control the plasma formation of Ag@TiO<sub>2</sub> core-shell nanofibers.

## Experimental Part

A mechanically scratched silver foil or a silver membrane (Sterlitech) was used as substrates for the experiments where Ag@TiO<sub>2</sub>-supported nanofibers were formed over increasing periods of time. The substrates were placed on a holder that could be rotated and heated by lamp irradiation. The maximum

temperature selected in the present work was 523 K. An SEM image of the utilized silver membrane has been previously reported.<sup>[17]</sup>

The plasma reactor used for deposition of TiO<sub>2</sub> consisted of a stainless steel chamber supplied with a microwave plasma source (SLAN, from Plasma Consult, GmbH, Germany) in a remote configuration. Details about this reactor can be found in ref. 18. For the deposition of TiO<sub>2</sub>, the reactor was supplied with oxygen ( $5 \times 10^{-3}$  mbar) and excited with a microwave power of 400 W. The Ti(OC<sub>3</sub>H<sub>7</sub>)<sub>3</sub> precursor was dosed by passing oxygen (2.7 sccm) through a stainless steel bottle that contained the precursor and was heated at 313 K. Both the line connecting this container with the chamber and the shower-like dispenser placed in the chamber were heated at  $T > 473$  K. This prevents any condensation of the precursor in the tubes. It is important to know that these plasma conditions yield rather compact and flat TiO<sub>2</sub> thin films when the substrate is quartz or a silicon wafer.<sup>[19]</sup> TiO<sub>2</sub> deposition experiments under these plasma conditions were also carried out on substrates that consisted of silicon wafers with small Ag or Pt particles deposited on their surface. These partially covered silicon substrates were prepared by sputtering from a silver target or by chemical vapor deposition from a Pt(acac)<sub>2</sub> precursor at temperatures between 643–693 K, followed by annealing at 873 K in an Ar atmosphere.<sup>[20]</sup> In the same experimental set-up, a silver foil at 130 °C was also exposed to an oxygen plasma for increasing periods of time. The plasma used in this case was similar to that used during deposition of TiO<sub>2</sub>, but without titanium precursor.

Some experiments were also carried out at much lower total pressures ( $\approx 10^{-4}$  mbar) by applying a magnetic field to the plasma source that was then working under electron cyclotron resonance (ECR) conditions.

XPS spectra were recorded in an ESCALAB 210 spectrometer working in the pass energy constant mode at a value of 50 eV. Spectra were excited with Mg K<sub>α</sub> radiation and the binding energy (BE) scale was referenced to the C 1s signal taken at 284.6 eV for the carbon that contaminated the surface of the samples. This carbon was adsorbed on the surface during the air handling and manipulation of the samples. The 'in situ' model experiments by plasma were carried out in a pre-chamber of the spectrometer where plasma and heating treatments could be carried out. After each plasma or deposition treatment the samples could be transferred to the analysis chamber without exposing them to air. Plasma treatments or depositions were carried out simultaneously on a Ag foil and a silicon wafer used as substrates. Before the deposition experiments, the substrates were cleaned by a mild sputtering with Ar<sup>+</sup> ions (1 000 eV) until no significant traces of carbon and/or oxygen could be detected by XPS. The cleaned foil (and the silicon substrate) was then exposed to a plasma of oxygen at 130 °C for 30 min. The oxidized substrate was then used to study the initial stages of deposition of TiO<sub>2</sub> on its surface by XPS. The plasma source used for these experiments consisted of a quartz tube where the plasma was excited by means of a resonant cavity connected to a microwave generator. The power was 70 mW and the oxygen was supplied to the tube up to a pressure of  $1.3 \times 10^{-1}$  mbar. The Ti precursor was dosed by bubbling oxygen through the Ti precursor under similar conditions as in the SLAN system. The oxygen plus precursor flow was dosed through a

heated valve and a tube ending 2 cm above the sample position. The amount of deposited titanium was controlled by adjusting the valve. To be able to follow the deposition process by XPS, very low growing rates were required in this experiment.

SEM analysis of different specimens was carried out in a Hitachi S5200 field emission microscope. Different sets of samples have been examined by this technique. They include Ag@TiO<sub>2</sub> nanofibers formed on the surface of the silver membrane, the plasma oxidized silver foil, and a TiO<sub>2</sub> layer formed on the silicon wafer with pre-deposited silver or platinum particles. The samples were examined without any specific manipulation. For TEM analysis of the individual fibers, they were separated from the substrates by sonication in ethanol for 3 min. The separated fibers that appeared floating on the surface of the liquid were collected with the typical copper grids used for TEM analysis. The TEM microscope was a Philips CM200 supplied with EDAX (X-ray emission). OES analysis of the plasma during deposition conditions was carried out by means of a suitable spectrometer ( $\frac{1}{2}$  M Digikröm). The signals were collected with an optical fiber positioned at the level of the plasma source through the ventilation holes that give access to the quartz jar where the discharge is produced.

## Results and Discussion

### Surface Reshaping of Silver Substrates Exposed to Oxygen Plasmas

The interaction of silver with oxygen plasmas is a well-studied subject because of the use of this metal for separation of atomic oxygen in atomic oxygen sources.<sup>[21]</sup> In an earlier work, Bhan et al.<sup>[22]</sup> reported that a silver foil exposed to an oxygen plasma underwent chemical (i.e., oxidation) and morphological transformations that result in a complete change in its surface topography. These changes were attributed to the flaking of the outmost surface layers of the substrate when they were fully oxidized by the plasma. In the present investigation we have investigated the morphological effects produced on the surface of a silver foil by the interaction with a plasma of oxygen. We used the same experimental plasma set-up as for the deposition of TiO<sub>2</sub> on the silver membrane. Figure 1 presents a series of SEM micrographs taken for a silver foil exposed at 130 °C to an oxygen plasma for increasing periods of time. The sequence of images a) to c)

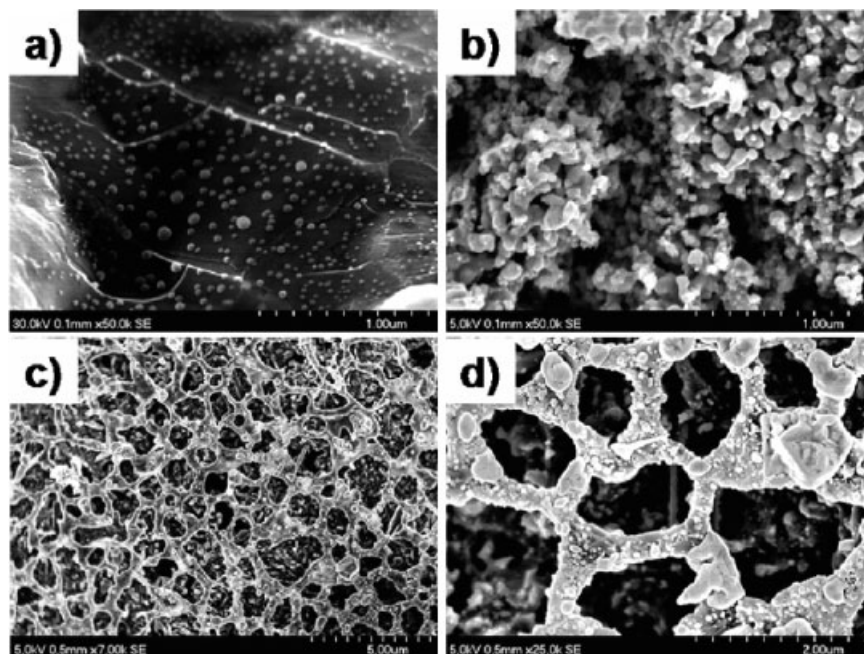


**Figure 1.** SEM micrographs from a silver foil after different times of oxygen plasma treatment at 130 °C. a) 20 min exposure, b) 60 min exposure, c) 120 min exposure, and d) high magnification image from sample (c).

clearly indicates that the surface topography becomes dramatically altered upon exposure to the plasma. This alteration consists of an increased roughening that ends in the formation of large and open domains, which suggests some kind of melting behavior of the surface. In the final images, the oxidized silver surface adopts a honeycomb-like structure, likely because this arrangement presents a minimum in surface free energy. Clearly, these images indicate that besides flaking, reshaping of the surface occurs as a result of the exposure of the silver foil to the oxygen plasma at 130 °C.

### Diffusion of Silver during TiO<sub>2</sub> Deposition

The possibility that silver atoms and/or clusters diffuse when a silver substrate is exposed to an oxygen plasma at 130 °C during deposition of TiO<sub>2</sub> was confirmed with an XPS model experiment. This experiment simulates the conditions that exist during the formation of Ag@TiO<sub>2</sub> nanofibers. It consisted of the simultaneous plasma deposition of TiO<sub>2</sub> in the pre-chamber of the XPS spectrometer onto a silver foil and a silicon substrate. Previously, the two substrates had been exposed to a plasma of oxygen as described in the experimental section. The formation of TiO<sub>2</sub> (i.e., Ti<sup>4+</sup> species) was proved on both the silver and silicon substrates by the detection of a majority Ti 2p<sub>3/2</sub> signal at a BE of 458.5 eV.<sup>[23]</sup> In addition, on the

silver substrate at room temperature a small contribution as a shoulder at 455.2 eV was observed only during the initial stages of deposition. This shoulder at relatively low BE is an indication of the formation of some  $Ti^{3+}$  species.<sup>[23]</sup> The  $Ti^{4+}/Ti^{3+}$  ratio deduced from the analysis of the spectra was 1.7. To assess the possible diffusion of silver during  $TiO_2$  deposition we followed the evolution of the intensity of the Ti 2p, Si 2p, and Ag 3d spectra as a function of the deposition time. As it is shown in Figure 2, when the deposition was carried out at room temperature, the Ti 2p/Si 2p and Ti 2p/Ag 3d atomic ratios determined from the area of the corresponding photoemission peaks continuously increased with deposition time. However, when the deposition was carried out at 130 °C, the Ti 2p intensity increased on silicon, but remained practically unmodified (i.e., almost no intensity of titanium) on silver. Moreover, after the experiment for the longest deposition time, some cracks were observed by SEM analysis on the surface of this sample. This precluded continuing with this deposition experiment for longer deposition times. At 130 °C the different evolution on the two substrates of the Ti 2p intensity is compatible with two different processes. One process is the diffusion of  $TiO_2$  into the bulk of silver. Another one is the diffusion of the silver or silver oxide to

cover the small particles of the titanium oxide formed at the earlier stages of deposition. Taking into account the previous SEM analysis of the plasma oxidized foil (cf. Figure 1), it is believed more likely that at 130 °C silver is diffusing to cover the  $TiO_2$  nuclei. In this way the deposited titanium oxide would not be accessible to the analysis by a surface sensitive technique like XPS.

### Preferential Growth of $TiO_2$ on Metal Particles

Very recently Ostrikov,<sup>[24]</sup> when discussing the potentialities of plasma deposition as a tool for the preparation of nanostructured layers, stressed the importance of the plasma sheath formed at the surface of the substrate as a directional vector that favours the preferential development of such nanostructures. Texturing of oxide thin films prepared by plasma deposition is a known phenomenon widely studied in the literature.<sup>[25]</sup> This seems particularly evident during the formation of supported carbon nanotubes by plasma deposition, although in this case the role of a metal catalyst is also essential.<sup>[10–12]</sup> In connection with these ideas we have checked the possibility that similar nanostructuring phenomena may appear when deposition is carried out on a silicon wafer with deposited silver or other metals particles. With this purpose, we report here some preliminary results concerning the microstructure of a  $TiO_2$  layer deposited by PECVD on this type of heterogeneous substrate. Figure 3, shows some selected SEM micrographs recorded for  $TiO_2$  deposited at 130 °C on Pt/silicon (Figure 3a,b) and Ag/silicon (Figure 3c–e) substrates. Two micrographs taken for the deposition carried out simultaneously on a bare silicon wafer are also presented for comparison (Figure 3f,g). The Pt deposited on the silicon substrates forms big and continuous aggregates that leave uncovered large zones of the substrate (Figure 3b). Meanwhile, the silver is in the form of small isolated particles with a wide distribution of sizes. In this case, although the total area free from metal is equivalent, the size of the zones without metal is relatively smaller (Figure 3e). The cross section view in Figure 3a clearly shows that the  $TiO_2$  grows preferentially on the Pt particles where it develops open and tilted columnar structures that produce the shadowing of the free zones of the substrate. This type of microstructure contrasts with that of the homogenous and columnar layer obtained on the silicon substrate during a similar deposition experiment (cf. Figure 3f,g). The preferential growth of the  $TiO_2$  on the metal structures was also confirmed by fluorescence analysis with the SEM microscope (i.e., EDX analysis). From the intensity of the Ti, Si, and Pt signals it was deduced that the Ti/Si atomic ratio measured on the substrate zones free from metal (i.e., 0.16) was smaller than the Ti/(Si + Pt) atomic ratio measured on the zones with metal particles (i.e., 0.17). Preferential deposition on the

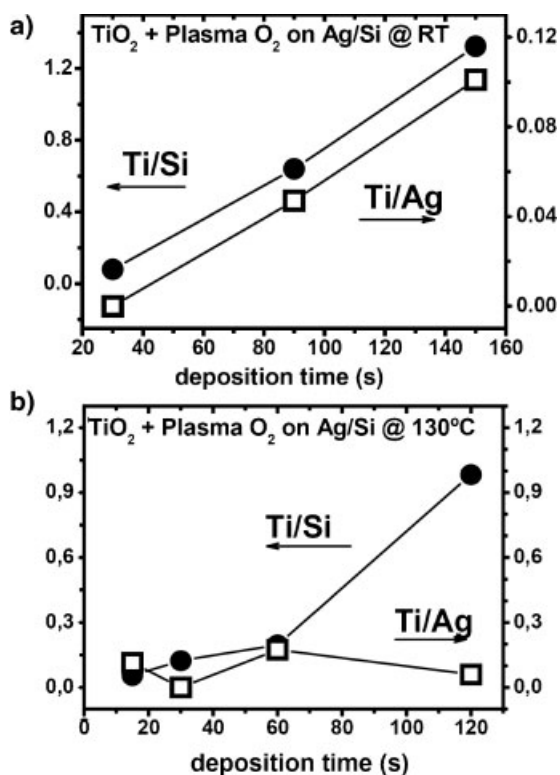
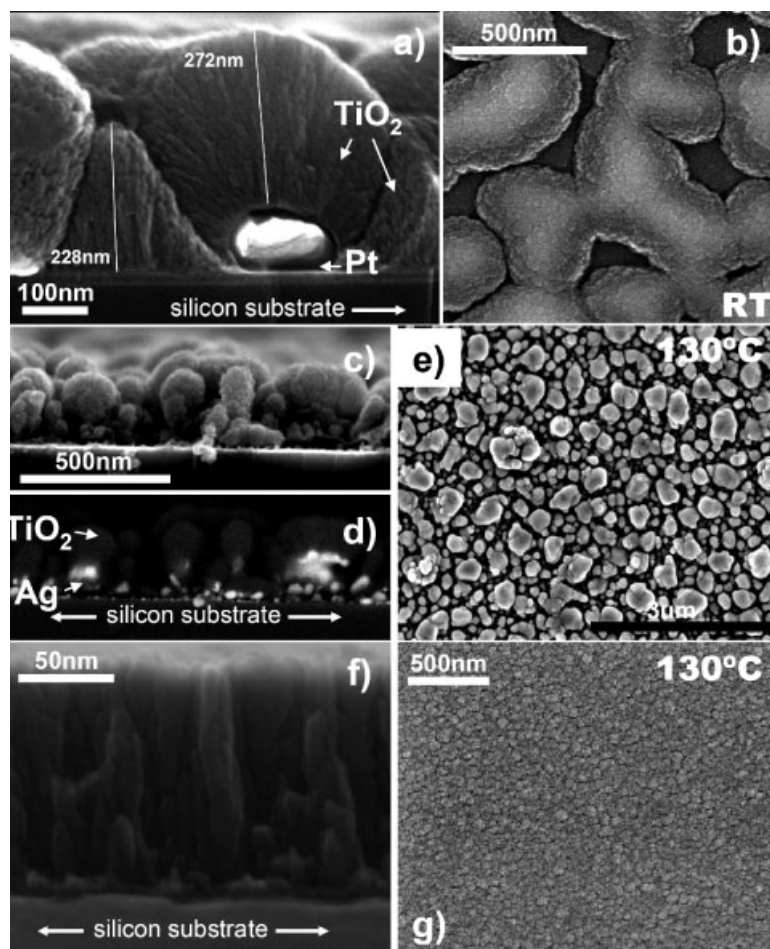


Figure 2. Ti 2p/Si 2p and Ti 2p/Ag 3d atomic ratios versus deposition time for  $TiO_2$  deposited on a silicon wafer and an oxidized silver substrate. a) Deposition at room temperature. b) Substrates at 130 °C during deposition.



**Figure 3.** Cross section (left) and normal (right) SEM micrographs for TiO<sub>2</sub> deposited at 130 °C on heterogeneous substrates formed by Pt (a,b) or Ag (c–e) particles and similar structures previously deposited on a flat silicon wafer. Images f) and g) are taken for TiO<sub>2</sub> deposited on a bare Si substrate and are included for comparison. In image (a) TiO<sub>2</sub> and Pt are signalled by arrows, while the different height of the TiO<sub>2</sub> layer grown on the particles or on the bare zones of the silicon substrate is also indicated. Image (d), taken with backscattered electrons to highlight the metal particles, corresponds to the same zone as image (c).

metal particles was also found when the deposition was carried out on the substrate with Ag particles (cf. Figure 3c–e). In this case, the TiO<sub>2</sub> seems to grow exclusively on the metal particles (cf. Figure 3c,d), which constitute the origin from which the oxide structures develop. The fact that preferential deposition is favored on either of the two types of metal particles (Pt or Ag) supports that this phenomenon is not a chemically driven effect (i.e., catalytic effect), but a property related to the metallic character of the particles. Note that the silicon wafer used for these experiments was un-doped and was covered by a native layer of insulating silicon oxide of at least 1.5 nm thickness.

Experiments were also carried out at 250 °C. At this temperature the crystalline anatase phase of TiO<sub>2</sub> is formed during PECVD deposition.<sup>[19]</sup> The images in Figure 4, characterized by well-defined crystal shapes,

confirm that at 250 °C crystallization of the TiO<sub>2</sub> into anatase has taken place. Formation of crystalline TiO<sub>2</sub> was also confirmed by X-ray diffraction. The corresponding diagram consisted of a superposition of the diffraction peaks of metallic silver and those of the anatase structure of TiO<sub>2</sub>. Formation of well-crystallized anatase can be clearly seen in Figure 4e, which shows a separated image of a silver particle that has been removed from the substrate and that bears a cap of TiO<sub>2</sub> crystals attached to it. However, most interesting for the objectives of the present work is that the columns of anatase grow from the metal particles and that inter-particle zones of the substrate are either shadowed by these TiO<sub>2</sub> structures (cf. Figure 4a for the Pt/Si substrate) or just free from any TiO<sub>2</sub> (cf. Figure 4c and 4d for the Ag/Si substrate).

Tentatively, we attribute the observed preferential growth of TiO<sub>2</sub> on the metal particles to local

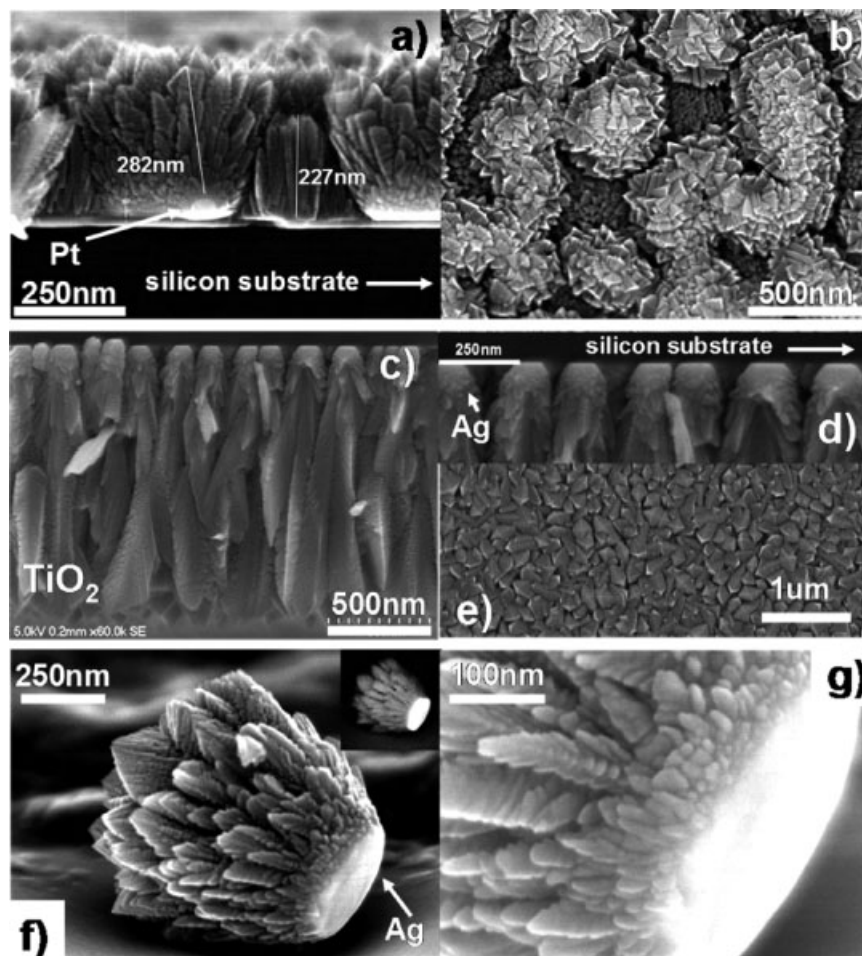


**Figure 4.** Cross section (a,c) and normal (b,e) SEM micrographs for  $\text{TiO}_2$  deposited at  $250^\circ\text{C}$  on heterogeneous substrates formed by Pt (a,b) or Ag (c–e) particles and similar structures previously deposited on a flat silicon wafer. Images (f) and (g) taken at two magnification scales correspond to a Ag- $\text{TiO}_2$  structure that has been removed from the substrate with the inset taken with backscattered electrons to highlight the presence of silver. Image (d) is an enlargement of image (c) to show that  $\text{TiO}_2$  exclusively grows on the silver particles. In these two latter images the substrate is at the top position of the frame.

inhomogeneities of the electrical field associated to the plasma sheath.

#### Fiber Development on Complex-Shaped Silver Substrates

In our previous work we have reported that Ag@ $\text{TiO}_2$  nanofibers grow at  $T > 130^\circ\text{C}$  during the plasma deposition of  $\text{TiO}_2$  on a corrugated silver substrate that had been previously oxidized by exposure to a plasma of oxygen.<sup>[17]</sup> To obtain a deeper insight into the mechanism of growth, here we analyse the growth process by taking images of the fibers formed over increasing periods of time. The effect of the temperature has also been analysed. Selected SEM images for three different deposition times (i.e., 45, 90, and 130 min) are shown in Figure 5. This experiment corresponds to the growth of nanofibers at  $130^\circ\text{C}$ . The set

of figures clearly evidence that long silver fibers covered by a thin skin of  $\text{TiO}_2$  are formed during the initial stages of  $\text{TiO}_2$  deposition (cf. Figure 5a,b). The length of the fibers does not increase significantly with the deposition time, but the thickness does (compare Figure 5a, 5c, and 5e on the one side and 5d and 5f on the other). This increase in thickness is because of the progressive deposition of  $\text{TiO}_2$ . It is also interesting that during the initial stages of deposition small silver particles grow on the  $\text{TiO}_2$  layer that covers some nanofibers (inset in Figure 5b). These silver particles disappear after a prolonged deposition of  $\text{TiO}_2$  (Figure 5c,d). A similar behavior was found when the experiment was carried out at  $250^\circ\text{C}$ , although in this case the  $\text{TiO}_2$  appears as small crystallites that grow around the central core formed by the thread of silver. Figure 6 shows a series of images taken for three different deposition times (i.e., 30, 90, and 160 min) at  $250^\circ\text{C}$  as

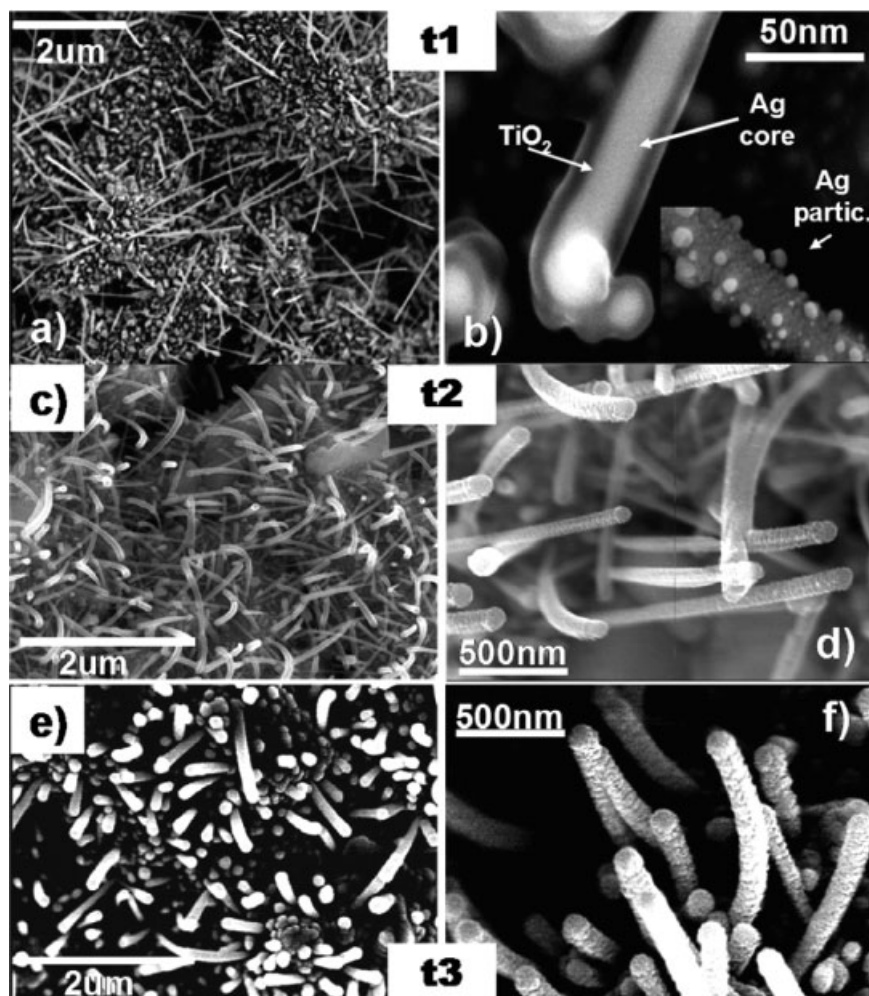


**Figure 5.** Normal SEM images for Ag@TiO<sub>2</sub> nanofibers plasma deposited at 130 °C for increasing periods of time ( $t_1 = 45$ ,  $t_2 = 90$ , and  $t_3 = 130$  min). Images have different magnification scales to show the high density of fibers formed on the substrate (left images) and their thickness and other morphological characteristics (right images). The inset in image (b) corresponds to a fiber with small silver particles on its surface; fibers of this kind are occasionally found at the beginning of the deposition.

substrate temperature. It is apparent in this figure that at 250 °C the thin Ag@TiO<sub>2</sub> fibers also increase in thickness while the silver core remains intact.

The proof that the centre of the fibers is formed by silver was obtained by TEM analysis. Figure 7 shows a TEM micrograph of an isolated fiber (Figure 7a) and the high-resolution image plus the electron diffraction diagram of its core (Figure 7b). It is clear from these images and the electron diffraction diagram that the silver core is a single crystalline thread with a FCC structure and a [110] preferential direction of growth.

### Plasma Characterization

To better understand the formation of the Ag@TiO<sub>2</sub> nanofibers by plasma deposition it is interesting to know

the type of species that are formed in the plasma during the decomposition of the titanium precursor. These species may act as primary 'building blocks' for the formation of the fibers and/or layers of TiO<sub>2</sub>. Analysis of the plasma under normal deposition and under ECR conditions (in this case leading to the formation of a slightly smaller concentration of fibers on the surface of the substrate) was carried out by OES. The corresponding spectra are shown in Figure 8. The spectrum under ECR conditions is reported to help in the identification of Ti related species which, in comparison, appear with lower intensity in the spectrum of the plasma at normal deposition conditions. The different peaks in these spectra have been assigned according to the literature<sup>[26–28]</sup> to different plasma species. Table 1 presents a summary of these species, which are also indicated in Figure 8. The most significant

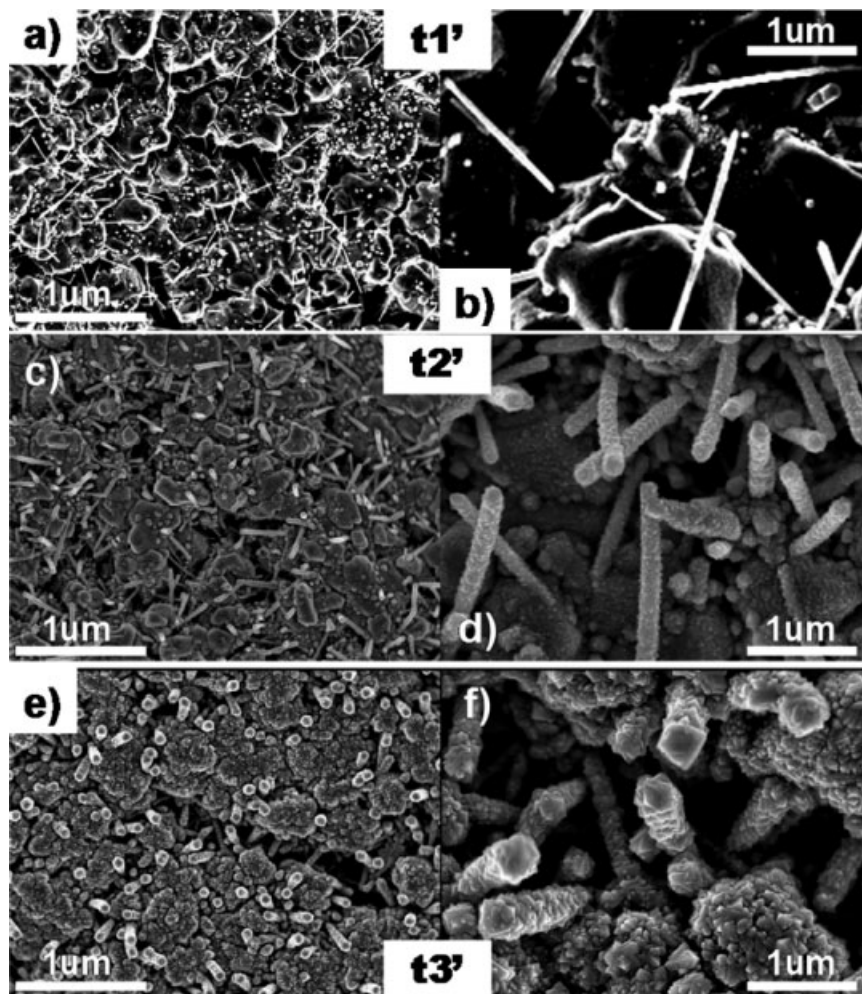


**Figure 6.** Normal SEM images for Ag@TiO<sub>2</sub> nanofibers plasma deposited at 250 °C for increasing periods of time from ( $t'_1 = 30$ ,  $t'_2 = 90$ , and  $t'_3 = 160$  min). Images have different magnification scales to show the high density of fibers formed on the substrate (left images) and their thickness and other morphological characteristics (right images).

feature with regard to our experiment is the formation in the plasma of Ti\* and TiO\* species. In addition, other species like H\*, CO\*, CO<sub>2</sub>\*, and CH\* are also detected (not marked in the figure). From this analysis, it seems likely that among the species that contribute to the growth of the Ag@TiO<sub>2</sub> fibers there are partially reduced species of titanium like Ti and TiO.

### General Discussion

The series of experiments described in the previous section can be rationalized to account for the mechanism of growth of Ag@TiO<sub>2</sub> nanofibers by PECVD.

The following basic phenomena have been evidenced by these experiments:

a) Mobilization of Silver. A silver foil substrate exposed to a plasma of oxygen experiences a change in the surface

topography of its outmost surface layers (cf. Figure 1a–d). When depositing TiO<sub>2</sub> by plasma on an oxidized silver substrate, silver tends to cover the TiO<sub>2</sub>, very likely because silver atoms and/or clusters migrate onto its surface (cf. Figure 2 bottom). Surface mobility of silver is enhanced at  $T > 130$  °C.

b) Preferential Growth of TiO<sub>2</sub> on Metal Particles. Plasma-deposited TiO<sub>2</sub> preferentially grows on metal particles. Rather than a catalytic effect of the metals, we tentatively associate this preferential growth to local inhomogeneities in the electrical field of the plasma sheath.

c) Growth of Ag@TiO<sub>2</sub> Nanofibers. Silver fibers grow very fast when TiO<sub>2</sub> is plasma deposited on an irregular silver substrate. These silver fibers are initially covered by a very thin layer of TiO<sub>2</sub>. When they reach a certain length they stop growing, while the thin TiO<sub>2</sub> layer continues to increase in thickness. At the initial stages

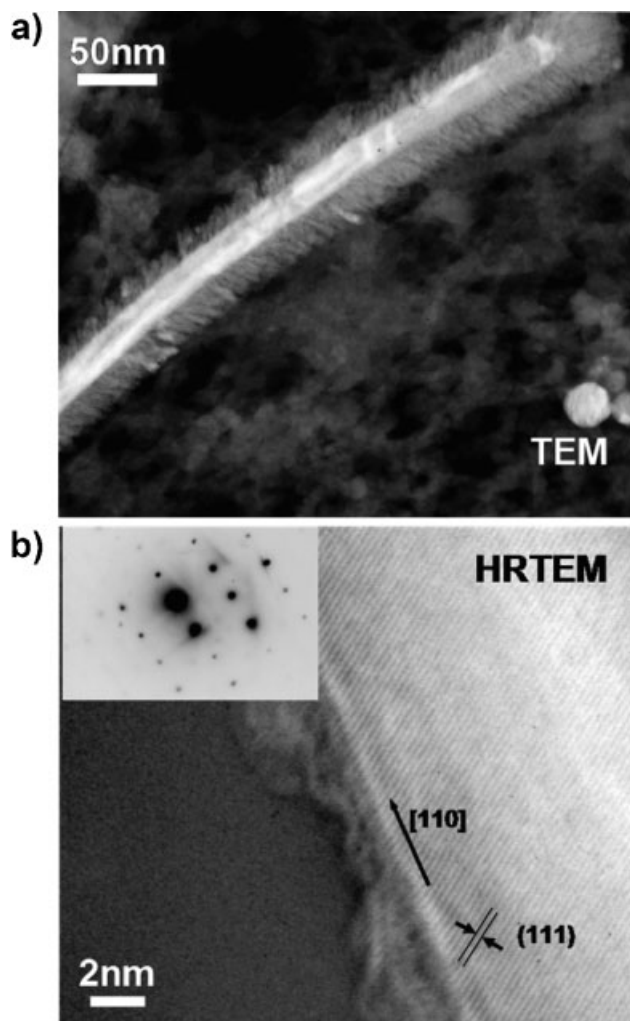


**Figure 7.** a) TEM image of a Ag@TiO<sub>2</sub> nanofiber formed after a short deposition time. b) High-resolution image and electron diffraction diagram (inset) of this fiber to prove its single crystalline character and its growth in the [110] direction.

of growth small silver particles appear on the surface of the external TiO<sub>2</sub> layer. These particles disappear when the deposition continues for long periods of time.

- d) During plasma deposition of TiO<sub>2</sub>, Ti and TiO species are detected in the plasma. These species are likely arriving at the surface where they contribute to the growth of the TiO<sub>2</sub> layer.

Based on characterization of the morphology of the Ag@TiO<sub>2</sub> fibers, we have previously proposed a 'volcano'-type mechanism to account for their growth. A scheme of this mechanism was reported in our previous publication.<sup>[17]</sup> This 'volcano'-type growth process assumes that metallic silver flows very rapidly from the basis of the fiber while the silver core is being covered by the TiO<sub>2</sub> layer. The

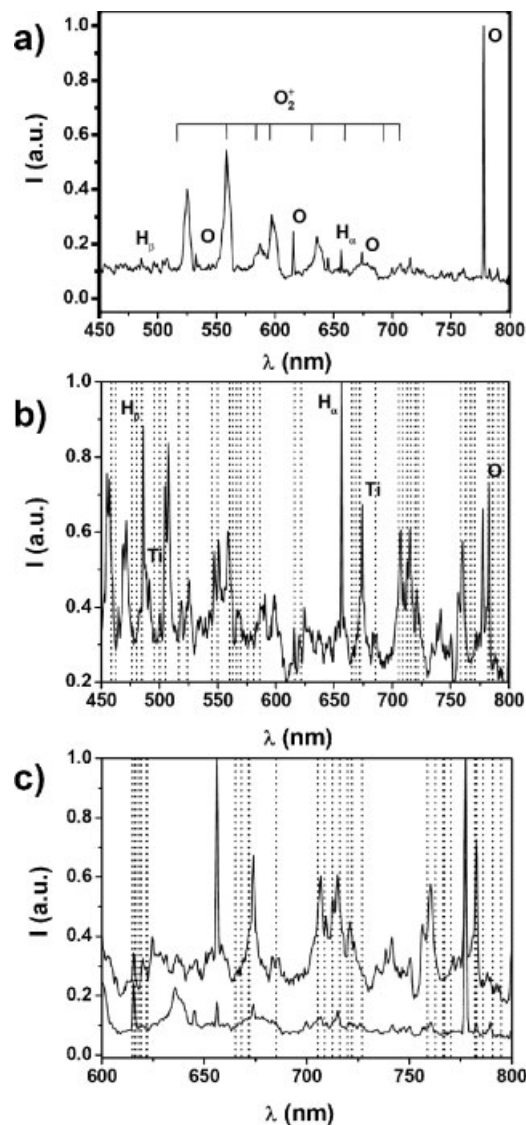


**Figure 8.** Normalized OE spectra of the plasma during deposition of TiO<sub>2</sub> for different plasma conditions as indicated. Dashed lines show the position of the band heads of TiO species. a) plasma under normal conditions of deposition. b) Plasma under ECR conditions. c) Comparison in an enlarged scale of higher resolution spectra corresponding to situations a) and b).

evidence summarized in points a)–d) supports this model and proves some of the basic hypothesis of the growth mechanism. Thus, the behavior of the plasma oxidized silver, the species detected in the plasma, and the preferential growth of titanium oxide on metal particles suggests a combination of the following effects during the fiber formation:

#### Silver Mobilization

The high mobility at  $T > 130^\circ\text{C}$  of plasma oxidized silver sustains the possibility that it can flow to the basis of the fiber. In this way, fibers may grow upward by additional

**Table 1.** Attribution of the main species detected in the plasma during deposition of TiO<sub>2</sub> under the different conditions of work.

Plasma	Species	Wavelength(s)		Transition(s)
		nm		
O <sub>2</sub>	O*	436.82, 532.96, 615.60, 645.60, 777.42, 844.64		Several emission lines involving 3s and 3p states
	H*	486.13, 656.3		2p–4d and 2p–3d (Balmer series)
	Ti*	674.31		4s–4p
	O <sup>2+</sup>	Several band heads		First negative system of O <sub>2</sub> <sup>+</sup> ions (b <sup>4</sup> Σ <sub>g</sub> <sup>-</sup> –a <sup>4</sup> Π <sub>u</sub> )
	TiO*	Small residual bands shadowed by the intense O <sub>2</sub> <sup>+</sup> bands		Same as by ECR
O <sub>2</sub> (ECR)	O*	436.82, 532.96, 615.60, 645.60, 777.42, 844.64		Several emission lines involving 3s and 3p states
	H*	410.17, 434.05, 486.13, 656.3		2p–6d, 2p–5d, 2p–4d, 2p–3d
	Ti*	334.20, 441.73, 455.55, 461.74, 462.31, 471.53, 498.17, 499.95, 549.01, 674.31, 868.30		Several emission lines
	O <sub>2</sub> <sup>+</sup>	Several band heads		First negative system of O <sub>2</sub> <sup>+</sup> ions (b <sup>4</sup> Σ <sub>g</sub> <sup>-</sup> –a <sup>4</sup> Π <sub>u</sub> )
	TiO	Several band heads, three triplet System in the visible region		Blue-green system: α, (C <sup>3</sup> Δ → X <sup>3</sup> Δ)  Orange-red system γ', (B <sup>3</sup> Π → X <sup>3</sup> Δ) Red system γ, (A <sup>3</sup> Φ → X <sup>3</sup> Δ)
	CO*	Several band heads		Triplet system
	CH*	Several band heads		431 system

supply of silver. The initial growth of the fibers is very fast and they may reach a maximum length 10 min after the beginning of the deposition process.

#### Stress in Plasma-Oxidized Silver Surfaces

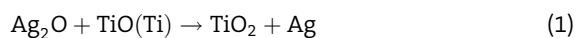
The experiment described in Figure 1 and 2, and previous others in the literature,<sup>[22]</sup> show that a silver surface subjected to plasma oxidation undergoes severe modifications of its morphology. These changes may even produce the flaking of their external layers. These modifications indicate that oxidation of silver at moderate temperatures introduces much stress in its outermost surface layers. Such an effect is to be expected by comparing the molar volumes of silver oxide and metallic silver, which are in an approximate ratio of 1:1.6:1.6 for Ag, Ag<sub>2</sub>O, and AgO, respectively. Therefore, we assume that the changes in the surface morphology of the silver foil (cf. Figure 1) provide a way to relax the extra surface stress induced by plasma oxidation in its structure. The formation of silver fibers on the silver membrane might also be a response to a surface relaxation process. In this way, the removal of surface stress would be the thermodynamic driving force that

favors the formation of the fibers. The silver fibers, all of them with a diameter of the order of 20–30 nm, are covered since the beginning of their formation by a TiO<sub>2</sub> layer (cf. Figure 5b). In a recent work by Liu et al.<sup>[29]</sup> about the structure of silver nanofibers, these authors developed a thermodynamic model that related the stability of the fibers with their diameter and their crystallographic structure. A minimum in their free energy of formation was found for silver fibers of 25.5 nm in diameter and a 4H structure. The fact that the surface free energy of 4H fibers is smaller than that of the more common FCC structure seems to be the main energetic factor favoring the formation of 4H silver fibers when they are very thin (i.e., for  $d < 50$  nm). In contrast, the single-crystalline silver core of our Ag@TiO<sub>2</sub> fibers present an FCC structure,<sup>[17]</sup> despite that its diameter of ≈20 nm is similar to that of the 4H fibers of Liu et al.<sup>[29]</sup> We believe that the fact that the silver thread is covered by a TiO<sub>2</sub> layer is critical for the stabilization of the FCC structure. This layer would contribute to a decrease of the surface free energy of the silver thread that, in this way, may crystallize into that structure.

The inset of Figure 5b also shows that at the beginning of their formation some the composite fibers present small silver particles deposited on the external TiO<sub>2</sub> layer. Although the fate of these silver particles is still unclear when the thickness of the TiO<sub>2</sub> continues to increase, a possibility is that silver atoms and/or clusters diffuse through the pores of the TiO<sub>2</sub> layer to join the silver core. Alternatively, these particles may disappear because they diffuse back to the silver substrate.

#### Chemical Reduction of Silver Oxide

After plasma oxidation and before the TiO<sub>2</sub> deposition, the surface of the silver substrate must consist of a mixture of silver oxides.<sup>[30,31]</sup> However, the core thread of the fibers consists of a single crystal of metallic silver. To account for the formation of metallic silver in the presence of a plasma of oxygen we claim a reaction of the type:



where Ti and TiO species have been detected in the plasma (Figure 8 and Table 1). Note that Reaction (1) does not discard other similar reduction reactions that involve species like CH\*, H\*, or CO\* also detected by OES spectroscopy (cf. Table 1). Besides providing a mechanism for the formation of metallic silver, Reaction (1) would also contribute to the preferential growth of titanium oxide on metallic particles as evidenced by the experiment described in Figure 3 and 4 and discussed in the next section.

#### Preferential Growth of TiO<sub>2</sub> on Metal Particles and Role of the Plasma Sheath

Our experiments have revealed that fibers have some preference to grow in the borders of hollows of the silver membrane used as substrate. The reasons why fibers preferentially grow in inhomogeneous substrates (see, for example, Figure 5a and 6f) are complex and not yet completely clarified. Ostrikov,<sup>[24]</sup> in a recent review about the use plasma techniques for the development of nanostructured materials, claimed that inhomogeneities in the electrical field of the plasma sheath may act as a driving force for the growth of nanostructures. For example, this would be one of the factors that contribute to the growth of carbon nanotubes by plasma deposition.<sup>[10–12]</sup> In other oxide, nitride, and complex carbon systems, formation of high aspect ratio nanostructures have also been found under different plasma conditions.<sup>[32–34]</sup> Model calculations accounting for the effect of an inhomogeneous electrical field of the plasma sheath are also available in the literature.<sup>[35]</sup> Inhomogeneities of the plasma sheath might also be important in our experiment as suggested by the fact that Ag@TiO<sub>2</sub> nanofibers preferentially grow at the edges or voids of the inhomogeneous silver substrate.

At these points it is likely that the electrical field associated with the plasma sheath presents a singular behavior. Similarly, the preferential growth of TiO<sub>2</sub> on metal particles deposited on a flat silicon wafer also points to a specific effect associated to the plasma sheath (cf. Figure 3 and 4). Very likely such a preferential growth is a result of a driven effect because of local inhomogeneities of the electrical field of the plasma sheath appearing on top of the particles.

#### Crystallization of the TiO<sub>2</sub>

Fibres formed by a silver core surrounded by small crystallites of anatase develop when the TiO<sub>2</sub> deposition is carried out at 250 °C (cf. Figure 6). This result indicates that formation of the fiber nuclei does not depend on whether the TiO<sub>2</sub> is amorphous or crystalline and confirms the importance of the TiO<sub>2</sub>/Ag interface interactions for the development of the composite fibers. A similar effect is suggested by the SEM micrograph images in Figure 4 that correspond to TiO<sub>2</sub> deposited on a silicon wafer with previously deposited metallic particles.

#### Description of the 'Volcano'-Type Mechanism

A summary of the different factors that contribute to the formation of the Ag@TiO<sub>2</sub> nanofibers is presented in the form of a scheme in Figure 9. This cartoon depicts a description of the volcano-type mechanism proposed in ref. 17. According to this scheme, surface inhomogeneities of the oxidized silver surface can act as nucleation centres where the electrical field of the plasma sheath would favor the deposition from ionized species of the plasma. In these points, chemical processes such as (1) or similar would be favored, which leads to the formation of metallic silver nuclei that are immediately covered by TiO<sub>2</sub>. Under deposition conditions, these nuclei serve as points to relax the stress accumulated by the silver oxide overlayer through the formation of the silver fibers. As indicated in this scheme, growing of the fibers is further favored by the inhomogeneities of the electrical field of the plasma sheath at the fiber tips. The process continues up to the complete release of the stress accumulated in the silver oxide overlayer.

#### Conclusion

The different experiments carried out here reveal that the formation of Ag@TiO<sub>2</sub> composite fibers is a complex process that can be tentatively explained by a combination of effects. Among them we have pointed out the importance of the mobility of the silver, the existence of

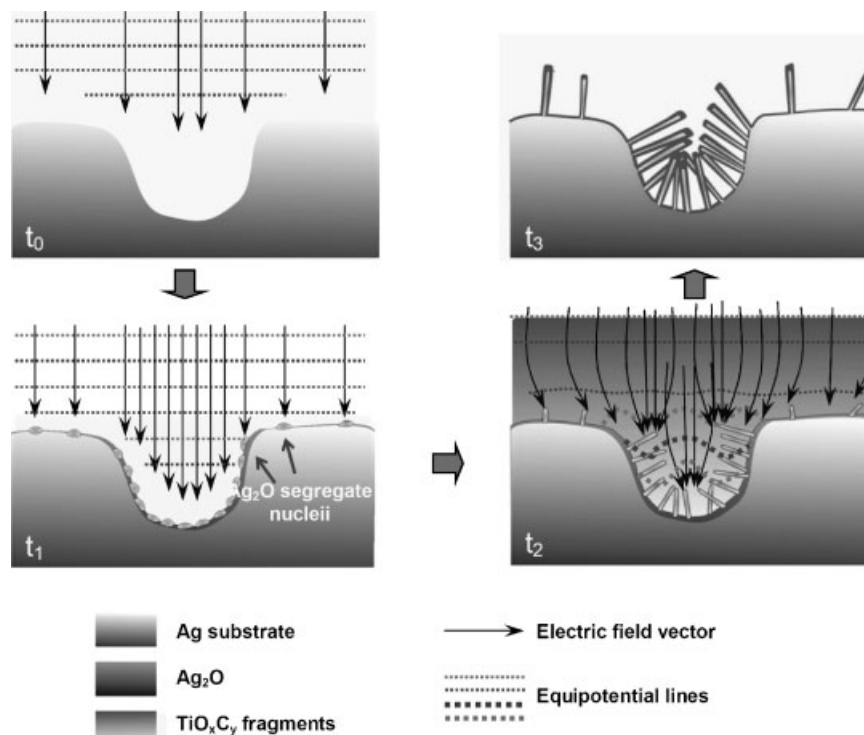


**Figure 9.** Representation of the different stages of the 'volcano'-type mechanism of formation of the Ag@TiO<sub>2</sub> nanocomposite fibers and the possible effect of the inhomogeneities of the electrical field of the plasma sheath in their formation.

inhomogeneities in the electrical field of the plasma sheath, and the reduction of silver oxide by intermediate species of titanium formed in the plasma. Although much work is still necessary to understand completely all these effects, we believe that these basic phenomena may have a general character and be applied for other materials. In this sense, we believe that similar approaches by plasma deposition could be used for the formation of other supported oxide nanofibers under moderate temperatures of deposition. Work is in progress in our laboratory to prove and generalize these ideas.

**Acknowledgements:** We thank the *EU* (project 032583) and the *Spanish Ministry of Science and Education* (project MAT2004-01558) for financial support. We also thank *T.C. Rojas* (ICMSE) for her assistance during the TEM characterization.

Received: February 6, 2007; Revised: May 3, 2007; Accepted: May 9, 2007; DOI: 10.1002/ppap.200700013

**Keywords:** fibers; nanostructures; nanowires; plasma enhanced chemical vapor deposition (PECVD); silver; TiO<sub>2</sub>

- [1] S. Yoo, S. A. Akbar, K. H. Sandhage, *Adv. Mater.* **2004**, *16*, 260.  
[2] J. Joo, S. G. Kwon, T. Yu, *J. Phys. Chem. B* **2005**, *109*, 15297.

- [3] C. Dames, B. Poudel, W. Z. Wang, J. Y. Huang, Z. F. Ren, Y. Sun, J. I. Oh, C. Opeil, M. J. Naughton, G. Chen, *Appl. Phys. Lett.* **2005**, *87*, 031901.  
[4] P. Hoyer, *Langmuir* **1996**, *12*, 1411.  
[5] D. Gong, C. A. Grimes, O. K. Varghese, W. Hu, R. S. Singh, Z. Chen, E. C. Dickey, *J. Mater. Res.* **2001**, *16*, 3331.  
[6] G. H. Du, Q. Chen, R. C. Che, Z. Y. Yuan, L. M. Peng, *Appl. Phys. Lett.* **2001**, *79*, 3702.  
[7] T. Kasuga, M. Hiramatsu, A. Hoson, T. Sekino, K. Niihara, *Adv. Mater.* **1999**, *11*, 1307.  
[8] J. Du, J. Zhang, Zh. Liu, B. Han, T. Jiang, Y. Huang, *Langmuir* **2006**, *22*, 1307.  
[9] J. Zhou, Y. Ding, S. Z. Deng, L. Gong, N. S. Xu, Z. L. Wang, *Adv. Mater.* **2005**, *17*, 2107.  
[10] G. Zhong, M. Tachiki, H. Umezawa, T. Fujisaki, H. Kawarada, *Chem. Vap. Deposition* **2004**, *10*, 125.  
[11] K. B. K. Teo, S.-B. Lee, M. Chhowalla, V. Smet, V. T. Binh, O. Groening, M. Castignolles, A. Loiseau, G. Pirio, P. Legagneux, D. Pribat, D. G. Hasko, H. Ahmed, G. A. J. Amaratunga, W. I. Milne, *Nanotechnology* **2003**, *14*, 204.  
[12] H. S. Uh, S. S. Park, *Thin Solid Films* **2006**, *504*, 50.  
[13] X. Liu, X. Wu, H. Cao, R. P. H. Chang, *J. Appl. Phys.* **2004**, *95*, 3141.  
[14] M. Mozetic, U. Cvelbar, M. K. Sunkara, S. Vaddiraju, *Adv. Mater.* **2005**, *17*, 2138.  
[15] C. Ducati, E. Barborini, G. Bongiorno, S. Vinati, P. Milani, P. A. Midgley, *Appl. Phys. Lett.* **2005**, *87*, 201906.  
[16] M.-S. Hu, H.-L. Chen, Ch.-S. Shen, L.-S. Hong, B.-R. Huang, K.-H. Chen, L.-Ch. Chen, *Nat. Mater.* **2006**, *5*, 102.  
[17] A. Borrás, A. Barranco, F. Yubero, A. R. González-Elipe, *Nanotechnology* **2006**, *17*, 3518.

- [18] A. Barranco, J. Cotrino, F. Yubero, J. P. Espinós, J. Benítez, C. Clero, A. R. González-Elipe, *Thin Solid Films* **2001**, *401*, 150.
- [19] F. Gracia, J. P. Holgado, A. R. González-Elipe, *Langmuir* **2004**, *20*, 1688.
- [20] G. Batiston, R. Gerbasi, A. Rodríguez, *Chem. Vap. Deposition* **2005**, *11*, 130.
- [21] D. Wu, R. A. Outlaw, R. L. Ash, *J. Vac. Sci. Technol. A* **1996**, *14*, 408.
- [22] M. K. Bhan, P. K. Nag, G. P. Miller, J. C. Gregory, *J. Vac. Sci. Technol. A* **1994**, *12*, 699.
- [23] J. A. Mejías, V. M. Jiménez, G. Lassaletta, A. Fernández, J. P. Espinós, A. R. González-Elipe, *J. Phys. Chem.* **1996**, *100*, 16255.
- [24] K. Ostrikov, *Rev. Mod. Phys.* **2005**, *77*, 489.
- [25] R. Groenen, H. Linden, R. van Sanden, *Plasma Proc. Polym.* **2005**, *2*, 618.
- [26] R. W. B. Pearse, A. G. Gaydon, "The Identification of Molecular Spectra", 4th edition, Chapman and Hall, New York 1976.
- [27] W. L. Wiese, M. W. Smith, B. M. Glennon, "Atomic Transition Probabilities", National Bureau of Standards, Gaithersburg, MD 1966.
- [28] [http://physics.nist.gov/PhysRefData/ASD/lines\\_form.html](http://physics.nist.gov/PhysRefData/ASD/lines_form.html).
- [29] X. Liu, J. Luo, J. Zhu, *Nano Lett.* **2006**, *6*, 408.
- [30] R. Snyders, M. Wautelet, R. Gouttebaron, J. P. Dauchot, M. Hecq, *Surf. Coat. Technol.* **2003**, *174*, 1282.
- [31] F. X. Bock, T. M. Christensen, S. B. Rivers, L. D. Doucette, R. J. Lad, *Thin Solid Films* **2004**, *468*, 57.
- [32] M. Yan, H. T. Zhang, E. J. Widjaja, R. P. H. Chang, *J. Appl. Phys.* **2003**, *94*, 5241.
- [33] C. Mirpuri, S. Xu, J. D. Long, K. Ostrikov, *J. Appl. Phys.* **2007**, *101*, 0234312.
- [34] J. F. AuBuchon, L.-H. Chen, S. Jin, *J. Phys. Chem. B* **2005**, *109*, 6045.
- [35] I. Levchenko, K. Ostrikov, K. Keidar, S. Xu, *Appl. Phys. Lett.* **2006**, *89*, 033109.